1 *Type of the Paper (Article)*

2 **Dynamic Carbohydrate Supply and Demand Model of Vegetative Growth:**
3 **Response to Temperature, Light, Carbon Dioxide, and Daylength**

4 Martin P.N. Gent [1,*]

5 [1] Forestry and Horticulture, Connecticut Agricultural Experiment Station, New Haven CT

6 06504-1106, USA. E-mail: Martin.Gent@ct.gov.

7 **Abstract:** Predicting the growth response of seedlings from the environmental responses of

8 photosynthesis and metabolism may be improved by considering the dynamics of non-

9 structural carbohydrate, NSC, over a diurnal cycle. Attenuation of growth metabolism when

10 NSC content is low could explain why some NSC is conserved through the night. A

11 dynamic model, incorporating diurnal variation in NSC, was developed to simulate growth

12 of seedlings hour-by-hour. I compared predictions of this model to published growth and

13 NSC data for seedlings that varied according to temperature, light, day length, or CO_2.

14 Prolonged-darkness experiments showed a temperature dependent upper limit on the

15 respiration capacity. Respiration was attenuated as NSC was depleted. Furthermore, when

16 NSC was high at dawn, inhibition of photosynthesis could attenuate the accumulation of

17 NSC under low temperature, or high light, or high CO_2. These concepts were used to

18 simulate plant metabolism and growth rates and diurnal variation of NSC in tomato

19 seedlings under two light levels and various temperatures. Comparison of other results

20 using the same model parameters showed the dynamic model could predict results for

21 starch and starch-less plants, and when growth was affected by CO_2 enrichment and day

22 length.

23 **Keywords:** carbohydrate starvation; non-structural carbohydrate; photosynthesis; photosynthesis inhibition;
24 respiration; relative growth rate; structure; diurnal variation

25

26

27

28

29   **1. INTRODUCTON**

30   **Supply and demand**

31   Photosynthesis is the limiting factor in most crop growth models [1-4], but metabolism

32   may also limit growth. If one assumes that low temperature limits growth, relative to the

33   optimum for a specie of plant, then the temperature dependence of metabolism may become

34   a limiting factor under increasing CO_2 levels. In the range from 10 to 25°C, the demand for

35   carbohydrate increases exponentially with temperature. The growth response of lettuce

36   (*Lactuca sativa*) has a $\mathbf{Q_{10}}$=3.3 [5], and the extension of wheat leaves (*Triticum aestivum*)

37   has a $\mathbf{Q_{10}}$ that varies from 2.5 to 3.5 [6]. Growth appears to be limited at warm temperatures

38   for two reasons: a decrease in photosynthesis and an increase in respiration. The

39   temperature response of photosynthesis is concave, first increasing and then decreasing

40   with increasing temperature [7]. In the model of Farquhar, van Caemmerer, and Berry [8],

41   the loss of photosynthesis at temperatures above 40°C is due to a continuous decrease in the

42   ratio of CO_2 to O_2 binding, as well as a breakdown in the conversion of light to chemical

43   energy.

44   Recently, Ido Seginer and I developed a steady-state model [9] based on the hypothesis

45   that growth is the minimum of the supply of non-structural carbohydrate, NSC, from

46   photosynthesis, and the demand of NSC to synthesize new tissue. This model predicted the

47   effects of temperature and light on vegetative plants growing in a constant environment.

48   The model also simulated acclimation to temperature as a transient process under these

49   conditions. It provided a plausible interpretation of demand- and supply-limited growth

50   data, and could be used to demonstrate the difference between short-term effects of

51   temperature as a transient process, and long-term effects resulting in acclimation [10].

52   **Carbon starvation**

53   The NSC from photosynthesis during daylight hours is not fully consumed by

54   biosynthesis in the dark, because some NSC is observed at dawn even under warm

55   temperatures, where demand should exceed supply. This amount was defined as a required

56   reserve in the steady-state model [9]. Experiments done under prolonged darkness show a

57   decrease of respiration and NSC with time, and higher respiration due to higher NSC for

58   plants grown under higher light before darkness [11]. Carbohydrate reserves were depleted

59   within 48-h in *Pennisetum glaucum* [12] and *Zea mays* [13], while loss of proteins was

60   much slower. Respiration followed a decreasing pattern over several days in tomato

61   (*Solanum lycopersicon*) [14], and sugars were depleted within one day in excised tomato

62   roots, while starch and proteins fell more slowly [15]. As NSC decreased over two weeks,

63   dark respiration and leaf elongation rate fell in *Festuca arundinacea* [16]. A similar

64   response was seen in *Medicago sativa* [17]. These authors considered respiration as the sum

65   of maintenance respiration represented by an intercept (about 30% of maximum), and

66   growth respiration proportional to NSC. I propose that the consumption of NSC continues

67   in the dark, at a rate which decreases as NSC is consumed, and that this governs the growth.

68   **Photosynthesis inhibition**

69   Evidence suggests that high NSC tends to inhibit photosynthesis. The NSC still

70   available at dawn was negatively correlated with growth [18]. Net photosynthesis of Beet

71   (*Beta vulgaris*) was reduced by 15% as starch plus sugar content increased over a day [19].

72   Even when spinach (*Spinacea oleracea*) showed no intra-day variation of photosynthesis, a

73   significant inhibition was observed as NSC accumulated from one day to the next [20]. The

74   NSC in tomato leaves was considerably higher in spring than in winter [21], and this was

75   correlated with more inhibition of photosynthesis around noon time in the spring. I claim

76   sink inhibition is required to model growth and NSC metabolism in plants. There was

77   feedback inhibition of NSC on photosynthesis in the steady-state model [9]. It is not clear

78   whether this inhibition changes within the photoperiod or only from one day to the next.

79   **Starch-less mutants**

80   In starch-synthesizing plants, part of the NSC retained in the leaf as starch is

81   remobilized to export sucrose to other parts of the plant in the dark [22-24]. Two sets of

82   observations show that starch turnover is highly regulated. First, only a small amount of

83   starch is left in plants at the end of the night [19, 25, 26]. This implies that the rate of starch

84   accumulation in the light is coordinated with the rate of utilization during the dark. This

85   balance could be due to regulated export rather than photosynthesis, resulting in more

86   export when there is more NSC. Second, to provide carbon to support metabolism and

87   export during a long night, a larger proportion of the photo-assimilate is partitioned to

88   starch in short- compared to long-day conditions [25, 27]. Do these mechanisms contribute

89   to the stimulation of starch synthesis in short days when less carbon is available? The

90   sugars that accumulate in leaves during the day are depleted by rapid respiration in the first

91   part of the night to reduce growth in starch-less mutants of Arabidopsis (*Arabidopsis*

92   *thaliana)* [28, 29]. I wish to know if starch-less mutants regulate NSC metabolism to assure

93   some NSC is available for growth and respiration during the night.

94   **Seedlings compared to larger plants**

95   Seedlings tend to grow exponentially, as least for a few weeks, with all parts increasing

96   in a similar fashion. The relative growth rate of seedlings can be related to the environment.

97   There is no indication how much of the leaf, stem, and root biomass is involved in growth

98   of larger plants. To analyze growth for larger plants and for longer growing times than used

99   here, the relationships between photosynthesis, respiration, and plant growth must be

100   determined separately for each plant species.

101   **Objectives**

102   I develop a dynamic model to explain the variation in NSC over the diurnal cycle,

103   based on hourly rates of metabolism and response to NSC. This model does not include a

104   correction for nitrogen or any other nutrient. Such a model predicts the rate of NSC

105   metabolism in seedlings, along with maximum and minimum NSC over the day, in

106   response to various environmental conditions, such as light, temperature, CO_2

107   concentration, and day length. It may predict relative growth rates better than the steady-

108   state model [9]. I incorporate sink inhibition of photosynthesis in the model, and assume

109   that starch synthesis and breakdown provides sufficient NSC for growth and respiration

110   during both day and night.

111

112

113

114
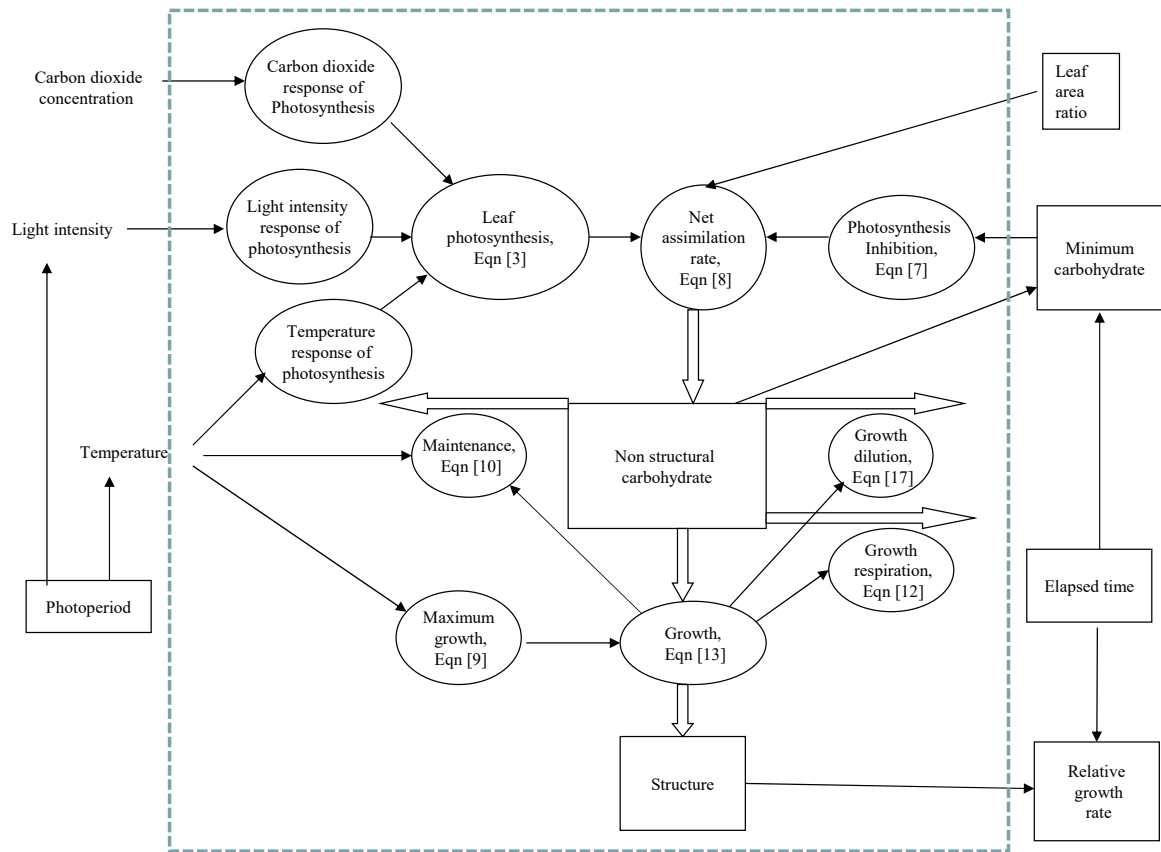
115

116   **2. MODEL DEVELOPMENT**

117

118   Figure 1. Schematic diagram of the hourly calculations of the dynamic model. Rectangles

119   indicate state variables. Those outside the calculation are daily variables. Ellipses indicate

120   rate equations. Text values are driving variables. The flow of NSC is indicates by thick

121   arrows. Influences on rate equations are indicated by thin arrows.

122

123   The model has two state variables: structural dry matter, $\mathbf{S}$, in g[SDM] m^{-2}[ground] and

124   non-structural dry matter, $\mathbf{C}$, in g[CHO] m^{-2}[ground] [10]. Figure 1 is a summary flow

125   diagram showing the state variables, rate variables, and driving variables (light,

126   temperature, $CO_{2)}$ of the model. The terms 'carbohydrate' and 'non-structural

127   carbohydrate', CHO and NSC, are considered as synonyms, and DM (dry matter) as a

128   general term, stands for both nonstructural, NDM, and structural, SDM, dry matter.

129   The differential (rate) equations are

130     $$\frac{\mathrm{d}\mathbf{S}}{\mathrm{d}t} = \mathbf{s} \tag{1}$$

131   and

132
$$\frac{dC}{dt} \equiv \mathbf{c} = \mathbf{p} - \mathbf{i} - \mathbf{m} - \mathbf{g} - \mathbf{s} - Cs \quad , \tag{2}$$

133   where $\mathbf{s}$ is structural growth rate and $\mathbf{c}$ is the rate of change of $\mathbf{C}$. Furthermore, $\mathbf{p}$ is

134   potential gross photosynthesis rate, $\mathbf{i}$ is inhibited photosynthesis, $\mathbf{m}$ is maintenance

135   respiration, and $\mathbf{g}$ is growth respiration, all in g[DM] m^{-2}[ground] h^{-1}. The parameters

136   mentioned here, and used later in the model, are defined in the appendix.

137   Photosynthesis is the only process that increases $\mathbf{C}$. I assume that potential

138   photosynthesis per unit lit leaf area, p, is a product of three functions, one of light, L (in

139   μmol[PAR] m^{-2}[leaf] s^{-1}), one of temperature, T (in K), and one of carbon dioxide

140   concentration, C_a (in μmol[CO$_2$] mol^{-1}[air]):

141
$$p\{L,T,\Gamma\} = P_{\max} f\{L\} h\{T\} k\{C_a\} = P_{\max} \left\lfloor \frac{L}{\gamma + L} \right\rfloor \left[1 - \kappa(T - \tau)^2 \left\lfloor \frac{C_a}{\delta + C_a} \right\rfloor \right] , \tag{3}$$

142   Where $\boldsymbol{P_{max}}$, in g[DM] m^{-2}[leaf] h^{-1}, is maximum photosynthetic rate and f, h and k

143   are dimensionless correction terms, all positive and smaller than one. This version is similar

144   to that of Gent and Seginer [9], with an extra term for CO$_2$. It fits the data of single leaf

145   photosynthesis of tomato under various conditions of light, temperature and CO$_2$ (data not

146   shown). Photosynthesis on a leaf area basis expressed in μmol[CO$_2$] m^{-2} [leaf]s^{-1} is

147   converted using the constant $10^{-6} * 30 * 3600$ into p in g[DM] m^{-2}[leaf] h^{-1}. Photosynthesis

148   per unit ground, $\mathbf{p}$, is obtained from p by multiplying by the sun-lit leaf area index, Λ (in

149   m^2[leaf] m^{-2}[ground]), namely

150
$$\mathbf{p} = \Lambda p = \Lambda P_{\max} f\{L\} h\{T\} k\{C_a\} . \tag{4}$$

151   Λ itself may be calculated for small plants with all leaves illuminated from a measured

152   value of the structural leaf area ratio, λ, (in m^2[leaf] kg^{-1}[SDM]), and $\mathbf{S}$:

153
$$\Lambda = \lambda \mathbf{S} \quad , \tag{5}$$

154   where I assume a constant leaf area ratio for seedlings.

155   Hence Eq. (4) becomes

156
$$\mathbf{p} = \lambda \mathbf{S} P_{\max} f\{L\} h\{T\} k\{C_a\} . \tag{6}$$

157   I assume that photosynthesis is inhibited in proportion to the NSC available at dawn, as

158   in the steady-state model [9], namely

159          $\mathbf{i} = \beta \mathbf{p} \mathbf{C}_d$,   (7)

160   where $\mathbf{C}_d$ is NSC at dawn, and β (m^2[ground] g^{-1}[NSC]) is a positive constant smaller

161   than $1/\mathbf{C}_d$. Consequently actual photosynthesis, $\mathbf{p} - \mathbf{i}$, is

162          $\mathbf{p} - \mathbf{i} = (1 - \beta \mathbf{C}_d) \lambda \mathbf{S} P_{max} f\{L\} h\{T\} k\{C_a\}$ (8)

163   Metabolism leading to growth is limited by temperature as well as by NSC. Let $\mathbf{n}\{T\}$

164   be the maximum rate of metabolism at a given temperature, both conversion to structure

165   and all respiration. I assume this limit increases exponentially with temperature over the

166   entire range

167          $\mathbf{n}\{T\} \equiv \mathbf{m}\{T\} + \mathbf{g} + \mathbf{s} = \mathbf{n}_0 \lambda \mathbf{S} \exp\{\zeta T\}$,   (9)

168   where $\mathbf{n}_0$ (in g[DM] m^{-2}[ground] h^{-1}) is metabolism of a crop of size $\lambda \mathbf{S} = 1$ and at 0 ºC.

169   Maintenance is assumed to increase exponentially, except with a temperature response,

170   θ, that may differ from ζ,

171          $\mathbf{m}\{T\} = \mathbf{m}_0 \lambda \mathbf{S} \exp\{\theta T\}$.   (10)

172   Furthermore,

173          $\mathbf{n}\{T\} \geq \mathbf{m}\{T\}$.   (11)

174   Structural growth, $\mathbf{s}$, is proportional to growth respiration, $\mathbf{g}$, via the conversion

175   efficiency, ε, from carbon in photosynthate to carbon in structure,

176          $\mathbf{s} = \left(\dfrac{\varepsilon}{1-\varepsilon}\right)\mathbf{g}$.   (12)

177   At high temperature, when $\mathbf{n}\{T\}$ is much greater than $\mathbf{m}\{T\}$, growth is limited by α,

178          $\mathbf{g} + \mathbf{s} = \dfrac{1}{1-\varepsilon}\mathbf{g} = \alpha \mathbf{C}$.   (13)

179   Here α, in h^{-1}, the response of growth to NSC, appears to be dependent on photoperiod but

180   independent of temperature. In the light, α_L has a higher value than in darkness α_D. As long

181   as NSC is not completely depleted, growth continues to utilize NSC.

182        $$\mathbf{g} + \mathbf{s} = \min\{\alpha\mathbf{C}, \mathbf{n}\{T\} - \mathbf{m}\{T\}\}. \qquad (14)$$

183   If NSC is completely depleted while $\mathbf{p} < \mathbf{m}$, maintenance respiration is supported by

184   sacrificing structural material. In that case

185        $$\mathbf{m} = \mathbf{m}\{T\}, \qquad\qquad \mathbf{g} = \mathbf{0} \qquad \text{and } \mathbf{s} = \mathbf{p} - \mathbf{m} \text{ (negative growth).} \qquad (15)$$

186   To describe the variation in NSC over the diurnal cycle, $\mathbf{S}$ is normalized to 1 g[SDM]

187   after each iteration. This requires subtracting a term in $\mathbf{Cs}$, corresponding to the NSC lost in

188   this renormalization

189        $$\frac{d\mathbf{C}}{d\mathbf{t}} = -Cs. \qquad (16)$$

190   Given the states $\mathbf{S}$ and $\mathbf{C}$ of the crop at any point in time, and while $\mathbf{C} > 0$, the terms of

191   Eq. (2) may be calculated from equations (8), (10), and (14),

192        $$\frac{d\mathbf{S}}{d\mathbf{t}} \equiv \mathbf{s} = \varepsilon \ \min\{\alpha\mathbf{C}, \mathbf{n}\{T\} - \mathbf{m}\{T\}\} \qquad (17)$$

193   The rates $\mathbf{p}$ and $\mathbf{m}$ are unaffected by the level of $\mathbf{C}$ in eqn (2). Once the rates $\mathbf{c}$ and $\mathbf{s}$

194   are known, the next-step values of the states $\mathbf{S}$ and C may be calculated, and then the next

195   set of rates and so on.

196   The parameters for NSC and respiration are expressed in g [CHO] g^{-1}[SDM] h^{-1} (Table

197   1). The model was simulated in the VENSIM simulation language (Ventana Systems,

198   Harvard MA), starting with an arbitrary initial state. Five days of periodic weather resulted

199   in a transition to an almost periodic trajectory of $\mathbf{S}$ and $\mathbf{C}$. Relative growth rate on the fifth

200   day, RGR, was calculated from the sum of growth increments over each hour divided by

201   the elapsed time.

Table 1. Parameters used in the dynamic model to simulate growth and non-structural carbohydrate in various crops.

Reference			[14]	[11]	[9]	[30]	[31]	[18]	[27]
Parameter	Units	Symbol	Tomato	Bean	Tomato	Tomato	Arabidopsis	Melon	Soybean
Maximum photosynthesis	μmol CO_2 m^{-2} s^{-1}	P_{max}			36	45	45	45	45
Half maximum light	μmol[PAR] m^{-2} s^{-1}	γ			309	309	309	309	309
Half maximum CO_2	μmol mol^{-1}	δ			225	225	225	225	225
Temperature optimum for PS	^{o}C	τ			24	24	24	27	27
Decrease per K^{-2} from τ	^{o}K^2	κ			0.0013	0.0013	0.0013	0.0013	0.0013
PS inhibition factor	g[SDM] g^{-1} [CHO]	β			0.9	1.25	1.25	1.25	1.25
Total respiration at 0°C	mg[CHO] g^{-1} [SDM] h^{-1}	n_0	0.025	0.05	0.03	0.035	0.035	0.025	0.035
Exponential response of total	^{o}K^{-1}	ζ	0.11	0.11	0.11	0.11	0.11	0.11	0.11
Maintenance respiration at 0°C	mg[CHO] g^{-1} [SDM] h^{-1}	m_0	0.007	0.007	0.007	0.007	0.007	0.007	0.007
Exponential response of maintenance	^{o}K^{-1}	θ	0.0693	0.0693	.0693	0.0693	0.0693	0.0693	0.0693

Conversion efficiency	dmnl	ε	0.75	0.75	0.75	0.75	0.75	0.75	0.75
Growth in dark	h^{-1}	α_D	0.07	0.07	0.07	0.07	0.07	0.07	0.07
Growth in light	h-1	α_L			0.07	0.14	0.14* 0.28	0.14	0.14

* Values are 0.14 and 0.28 h^{-1}, for **COL0** and **pgm**, respectively.

1   **3. PARAMETER ESTIMATION**

2   Altogether the dynamic model has 14 parameters: $\boldsymbol{P_{max}}$, $\boldsymbol{\gamma}$, $\boldsymbol{\kappa}$, $\boldsymbol{\tau}$, $\boldsymbol{\delta}$, λ, $\boldsymbol{\beta}$, $\mathbf{n}_0$, $\boldsymbol{\zeta}$, $\mathbf{m}_0$, $\boldsymbol{\theta}$,

3   $\boldsymbol{\varepsilon}$, $\boldsymbol{\alpha_L}$, **and** $\boldsymbol{\alpha_D}$, as indicated in Table 1. As much as possible, the parameter values used were

4   equivalent to those for tomato in the steady-state model [9]. Values for $\boldsymbol{P_{max}}$, $\boldsymbol{\gamma}$, $\boldsymbol{\delta}$, $\boldsymbol{\tau}$, and $\boldsymbol{\kappa}$ in

5   Eqn. (3) were determined by least squares fit to data from measurement of gross

6   photosynthesis of tomato leaves [9], except data were measured at CO_2 concentrations of

7   200, 400, and 1600 µmol[CO_2] mol^{-1}[air] (data not shown). The regression between measured

8   and observed data was R^2=0.94 for this model, compared to a value of R^2=0.97 for the

9   Farquhar model [8]. A $\boldsymbol{P_{max}}$ value was found which optimized the prediction of growth rate

10 and NSC over all environments.   Leaf area ratio, usually reported per g [DM], was

11 transformed to λ, by subtracting NSC from the actual DM. The parameter $\boldsymbol{\beta}$ was chosen to

12 optimize the fit between observed and predicted NSC, when it accumulated at cool

13 temperatures. Maintenance respiration, $\mathbf{m}_0$, and its temperature dependence, $\boldsymbol{\theta}$, were

14 determined from observations of dark respiration of tomato leaves at various temperatures

15 [9]. This gave a $\boldsymbol{Q_{10}}$ = 2. The values of parameters describing metabolism, $\mathbf{n}_0$ and ζ, were

16 determined by fitting growth data at temperatures cooler than 20°C. The resulting $\boldsymbol{Q_{10}}$ = 3,

17 was different from $\boldsymbol{\theta}$ for maintenance. A value of 0.75 is used for $\boldsymbol{\varepsilon}$, the parameter related to

18 growth efficiency, based on the analysis of Penning de Vries et al. [35].

19   The parameter $\boldsymbol{\alpha}$, the response of growth to NSC, is a new element compared to the

20 steady-state model [9]. Growth and diurnal variation in NSC were sensitive to this parameter

21 at warm temperatures when $\mathbf{n}\{T\}$ did not limit metabolism. A lower limit to $\boldsymbol{\alpha_D}$ was set by the

22 growth rates observed under this condition. An upper limit was set by the minimum NSC

23 content observed, or by the magnitude of the diurnal variation of NSC. The dependence of $\boldsymbol{\alpha_L}$

24 in the light was given by the losses of NSC over the light period.

25

26 **4. RESULTS**

27 **Respiration in prolonged darkness**

28   Two studies followed respiration in prolonged darkness, to understand NSC use without

29 photosynthesis. Respiration in prolonged darkness was simulated for tomato plants (*Solanum*

30 *lycopersicon*) grown under high or low irradiance before being put in the dark [14]. Plants

31 under different irradiance were of different sizes, and they were converted to values per gram

32 SDM using a multiplier of 500 and 120 g/plant, for plants pre-treated at 1000 and 200

33 µmol[PAR] m^{-2} s^{-1} , respectively. Dark respiration for plants pre-treated at 1000 µmol[PAR]

34

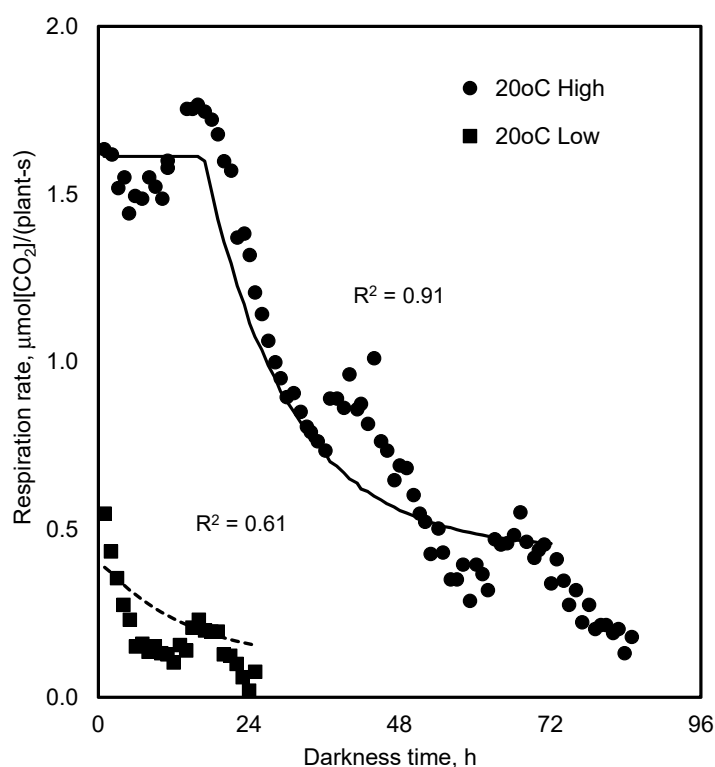35　Figure 2. Respiration rate of whole tomato plants in prolonged darkness after pre-treatment

36　under high or low light of 1000 or 200 μmol[PAR]m^{-2} s^{-1} [14]. Filled symbols are measured

37　values for high and low light, and empty symbols are predictions of the dynamic model. The

38　R^2 is given for each time series.

39

40　m^{-2} s^{-1} stayed on a plateau for 15 h before falling exponentially (Fig. 2). There was also a

41　small diurnal variation, similar to the light that plants received before being in darkness [14].

42　　　The model predicted values similar to those observed until 36 h. Model values were less

43　than observed for the next 12 h. Finally, the model predicted a level of respiration equivalent

44　to maintenance, 0.45 μmol/plant s^{-1} after 57 h, while actual values dropped to 0.2 μmol/plant

45　h^{-1} at 70 or 80 h. One parameter had to be changed relative another study of tomato seedlings

46　[9]. The value **n$_0$** was reduced from 0.035 to 0.025 mg[CHO] g^{-1}[SDM] h^{-1}. This reduced

47　growth respiration compared to seedlings. Plants pre-treated at 200 μmol[PAR] m^{-2} s^{-1} had

48　dark respiration that fell exponentially from 0.5 to 0.06 μmol/plant h^{-1} over 24 h. The model

49　predicted values would fall from 0.39 to 0.15 μmol/plant h^{-1} at 24 h, the value due to

50　maintenance respiration. The correlation between predicted and actual values of respiration

51　was R^2 = 0.91 under high light, and R^2 = 0.61 under low light, with **n$_0$** modified.
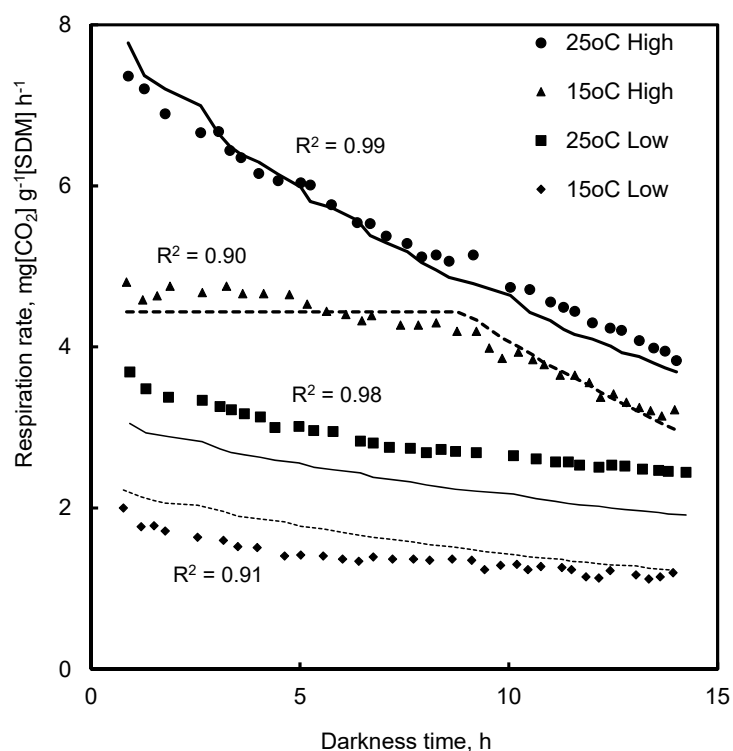
52

Figure 3: Respiration rate of bean plants in prolonged darkness after pre-treatment under high

or low light [11]. Filled symbols are values after pretreatment under high light at 25 and

15ºC, and under low light at 25 at 15ºC, from top to bottom, respectively. Empty symbols are

predictions of the dynamic model. The R^2 is given for each time series.

57

58   Respiration rate of bean plants (*Vica faba*) was followed for 14 h in darkness at 15 and

25ºC, after pre-treatment under high or low light [11]. For respiration, I used 1000 *

(maintenance + growth respiration), equivalent to $mg[CO_2]\ g^{-1}[SDM]\ h^{-1}$. For high-light

plants followed at 25ºC in darkness, dark respiration fell from 7.4 to 3.8 $mg[CO_2]\ g^{-1}[SDM]$

h^{-1} over 14 h (Fig. 3). Using a value of $\mathbf{n_0}$=0.05 and an initial NSC of 0.35 $g[NSC]\ g^{-1}[SDM]$,

the dynamic model predicted a similar decrease with time. For high-light plants followed at

15ºC in darkness, dark respiration was at a plateau of 4.7 $mg[CO_2]\ g^{-1}[SDM]\ h^{-1}$ for 9 h

before falling to 3.2 $mg[CO_2]\ g^{-1}[SDM]\ h^{-}$1. The model had similar predictions. I had to set

the initial NSC at 0.08 $g[CHO]\ g^{-1}[SDM]$ to get the model predictions under low light. Dark

respiration fell from 3.5 to 2.4 $mg[CO_2]\ g^{-1}[SDM]\ h^{-1}$ over 14 h for plants at 25ºC.   The

model predicted a similar trend with time, but offset by 0.5 $mg[CO_2]\ g^{-1}[SDM]\ h^{-1}$. Dark

respiration fell from 2.0 to 1.1 $mg[CO_2]\ g^{-1}[SDM]\ h^{-1}$ over 14 h for plants at 15ºC in

70 darkness. The model predicted a higher respiration at the beginning of darkness, but values

71 fell to those observed after 14-h. Using the adjusted values for n_0 and initial NSC, the

72 correlation between predicted and actual values ranged from $R^2 = 0.90$ to $R^2 = 0.99$ for all

73 series (Fig. 3).

74   Under high light, for tomato, and for bean at 15ºC, respiration in darkness was first

75 predicted to plateau, when growth respiration was governed by α_D, and then decrease with

76 time, when growth respiration was less than α_D. There was some uncertainty in the prediction

77 of maintenance respiration in tomato under prolonged darkness. This was not a concern when

78 the model was applied to plants under a normal diurnal cycle, as NSC never fell to zero.

79 **Effect of temperature and light**

80   Relative growth rates and NSC were predicted for tomato seedlings (Solanum

81 lycopersicon) grown in a constant environment under one of a range of temperatures, and

82 under low or high light, averaging 110 or 370 µmol[PAR]m^{-2} s^{-1} [30]. Values from the

83 steady-state model [9] were used to estimate parameters for the dynamic model, except that

84 they were converted into hourly rates. There is no "reserve carbohydrate" in the dynamic

85 model. Instead metabolism was slowed as NSC became depleted, as in Eqn. (13). Several

86 parameters of the dynamic model were changed with respect to the steady-state model. The

87 maximum photosynthesis rate, P_{max}, was increased from 36, in the steady-state model, to 45

88 µmol m^{-2} s^{-1}, because a greater fraction of the carbohydrate in the plant was considered when

89 predicting photosynthesis inhibition. The parameter relating NSC to photosynthesis

90 inhibition, β, was increased from 0.88 to 1.25 g[SDM] g^{-1}[CHO], going from the steady-state

91 to the dynamic model, to more closely predict NSC at low temperatures where it accumulated

92 to a high concentration. In part, this change was likely due to increased photosynthesis, which

93 would otherwise result in greater accumulation of carbohydrate at low temperatures.

94   The parameters describing rates of respiration and metabolism, such as maintenance

95 respiration, **m**, and the temperature dependence limiting growth demand, **s** in the steady-state

96 model and **n** here, did not need to be changed in the conversion from a steady-state (Table 1,

97 Column 3) to a dynamic model (Column 4). However, the meaning of the parameter, n_0,

98 changed. It set a limit for growth metabolism alone in the steady-state model, while in the

99 dynamic model, the limit was on the maximum rate at a given temperature of all metabolism,

100 including growth, Eqn. (9). A value of $n_0 = 0.035$ mg[CHO] g^{-1}[SDM] h^{-1} in the dynamic

101 model predicted growth rates very similar to the steady-state model (Fig. 4), but it also

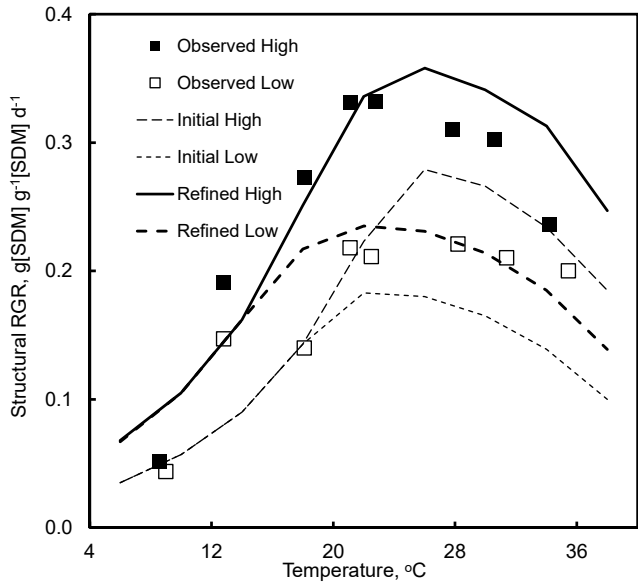102 increased NSC (Fig. 5). The correlation between predicted and actual values for relative

103

104   Figure 4. Relative growth rates observed for tomato seedlings over a range of temperatures

105   under low or high light, averaging 110 or 370 μmol[PAR]m^{-2} s^{-1} [30]. Observed values,

106   indicated by symbols, were compared with predictions, lines, from initial and refined

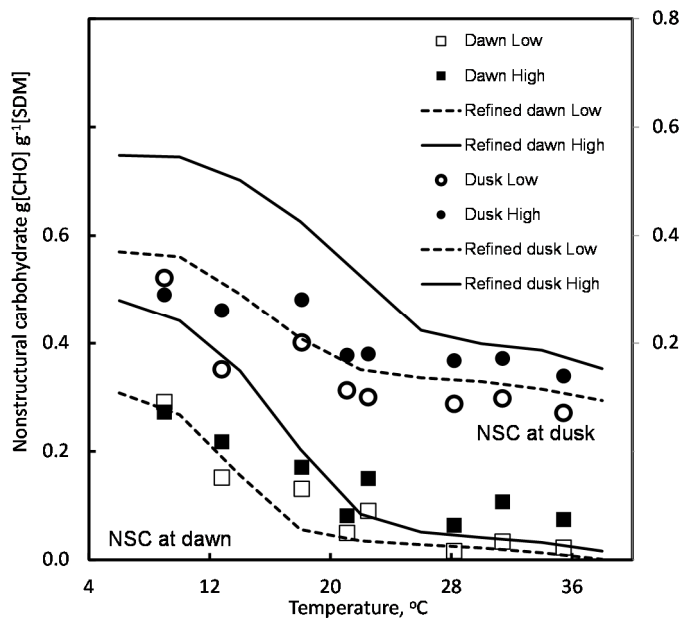107   versions of the dynamic model.

108

109

110   Figure 5. Non-structural carbohydrate at dusk and dawn in tomato seedlings grown over a

111   range of temperatures under low or high light, averaging 110 or 370 μmol[PAR] m^{-2} s^{-1} [30].

112   Values are offset for dusk and dawn. Symbols represent observed NSC. Predictions are from

113   the dynamic model using parameter values as specified for the refined model, lines.

114   growth rates was similar for the steady-state and the dynamic models, R2= 0.74 and R2=0.76,

115   respectively. The single value α_D = 0.07, derived from studies of changes in NSC and

116   respiration for mature tomato plants growing in prolonged darkness [14], was insufficient to

117   describe relative growth rates for the rapidly growing tomato seedlings [30]. When α was

118   constant the model predicted that NSC at the end of the day was higher than observed, while

119   NSC at the end of the night was lower than observed (data not shown). This was resolved by

120   allowing α to depend on photoperiod. Setting α_D in the night to one half α_L in the day, α_D =

121   0.07 h^{-1} and α_L = 0.14 h^{-1}, simulated the diurnal variation in NSC more accurately (Fig. 5). In

122   particular, NSC at low temperature was greater for the model than for the data, but the excess

123   NSC was less for the refined than for the initial model. The correlation between predicted and

124   actual minimum values of NSC, was greater for the refined than for the initial dynamic

125   model, R^2 = 0.83 and R^2=0.77, respectively. It was much greater that the correlation of

126   minimum values of NSC in the steady-state model (R^2=0.65).

127   **Starch and starch-less mutants of Arabidopsis**

128   NSC and growth were predicted for starch synthesizing and starch-less lines, **COL0** and

129   **pgm**, of *Arabidopsis thaliana* [31]. The NSC was observed for various times within a 24-h

130   cycle [31]. A single value of λ = 18.5 m^{-2} kg[SDM] was used as the leaf area ratio to fit the

131   data, along with the photosynthesis parameters for tomato. These parameters gave results in

132   agreement with data, when other model coefficients were the same as the refined values for

133   tomato, except for the starch-less mutant, α_D = 0.28 h^{-1}.

134   Predictions of NSC at dusk and dawn are given for plants with 6- to 20-h day lengths in

135   Table 3. For starch-synthesizing **COL0**, the dynamic model predicted NSC at dawn would

136   increase up to a 20-h day length. On the other hand, the dynamic model predicted very little

137   NSC in the starch-less mutant, **pgm**, while actual values remained near zero. The values

138   predicted at dusk for **COL0** agreed with measurements, except at a 16-h day length. There

139   was no variation predicted in the starch-less mutant at dusk, whereas the actual values of

140   NSC decreased as photoperiod increased. The decrease in NSC with increased day length was

141   not predicted by either the dynamic or by the steady-state model. The correlation between

142   actual values at dawn, and the values predicted by the dynamic model were R^2=0.90 and

143   R^2=0.03, for **COL0** and **pgm**, respectively. The minimum NSC from the steady-state model

144   applied to **COL0** had a poorer correlation, R^2=0.67. The growth rates were predicted to vary

145   with day length, but they varied little between **COL0** and **pgm** (Table 3). The starch-less

146   mutant was predicted to have faster growth under a longer photoperiod.

147

148 Table 3. Effect of photoperiod on non-structural carbohydrate available in starch type,

149 **COL0**, and starch-less, **pgm**, mutants of Arabidopsis. Observations are from Gibon et al. [31]

150 and predictions are from the dynamic model, including relative growth rate. R^2 is the

151 correlation between observed and predicted NSC.

|	Observed		Predicted		
	Non-structural	carbohydrate			Relative growth rate
Photoperiod	Dawn	Dusk	Dawn	Dusk	
h	g[CHO] g^{-1}[SDM]		g[CHO] g^{-1}[SDM]		g g^{-1} d^{-1}
	Starch type	**COL0**			
6	0.007	0.046	0.0	0.058	0.048
9	0.009	0.062	0.003	0.069	0.087
12	0.006	0.073	0.011	0.074	0.122
16	0.021	0.095	0.025	0.076	0.166
20	0.051	0.079	0.045	0.075	0.206
R^2			0.90	0.84	
	Starch-less	**pgm**			
6	0.002	0.058	0.0	0.038	0.047
9	0.002	0.047	0.0	0.041	0.086
12	0.003	0.041	0.001	0.041	0.126
16	0.004	0.024	0.009	0.041	0.175
20	0.002	0.012	0.022	0.040	0.220
R^2			0.03	0.22	

154
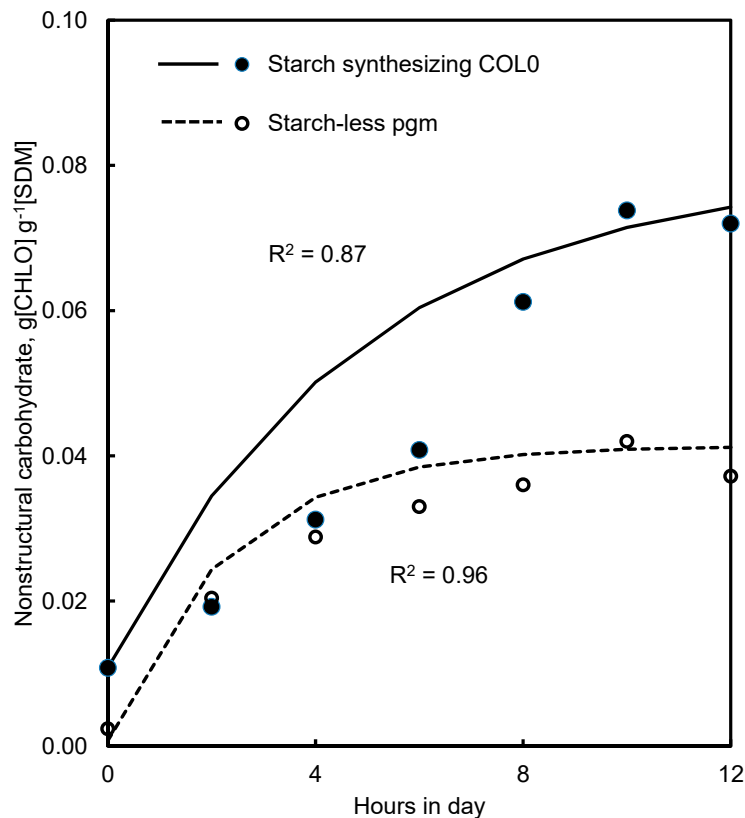
Figure 6. Non-structural carbohydrate in starch synthesizing, **COL0**, or starch-less, **pgm**,

mutants of Arabidopsis under a 12-h day length [31] and predictions of the dynamic model.

Symbols are data and lines are predictions.

Values of NSC were predicted for **COL0** and **pgm** under a 12-h day length (Fig. 6). The

dynamic model predicted values at 12-h that were similar to those observed. However within

the photoperiod, the predicted values of NSC were correct for **pgm**, but were underestimated

for **COL0** from 2 to 6 h. Both **COL0** and **pgm** had similar levels of NSC at 2 to 6 h, while

the model predicted more NSC for **COL0** than **pgm**. The correlation between predicted and

actual values was $R^2 = 0.87$ and $R^2 = 0.96$, for **COL0** and **pgm** mutants, respectively

Effect of CO_2 and Photoperiod

Diurnal variation in NSC was predicted for muskmelon (*Cucumis melo*) grown at 20 and

40°C day temperatures and at 300 and 1500 $\mu mol[CO_2]$ mol^{-1} [18]. Two parameters had to be

altered to more closely fit the data for melon, which was capable of metabolizing NSC to

levels much lower than found in tomato seedlings at 20°C. The relatively large difference in

NSC for plants grown at 20 and 40°C day temperature required $n_0 = 0.025$ mg[CHO] g^{-1}

$[SDM]$ h^{-1}. To better fit the difference in growth at 20 and 40°C, the optimum temperature

173   for photosynthesis, **τ**, was raised from 24 to 27℃. The model with these revised parameters

174   predicted slower growth for melon than tomato at cool temperatures, but faster growth at

175   warm temperatures.

176   The dynamic model accurately predicted the diurnal variation in NSC within muskmelon

177   plants, as well as the difference between the treatments, and the generally lower NSC in

178   melon compared to tomato. The highest NSC was predicted at 20℃ and 1500 μmol[CO_2]

179   mol^{-1} (Fig. 7). Presumably, the rate of metabolism at 20℃ was not sufficient to convert this

180   NSC to structural growth. Under 300 μmol[CO_2] mol^{-1}, the NSC was not sufficient for rapid

181   growth at either 20 or 40℃. The fastest growth at 1500 μmol[CO_2] mol^{-1} was predicted at

182   40℃, 0.24 g g^{-1} d^{-1}, compared to 0.21 g g^{-1} d^{-1} at 20℃. The correlation between predicted and

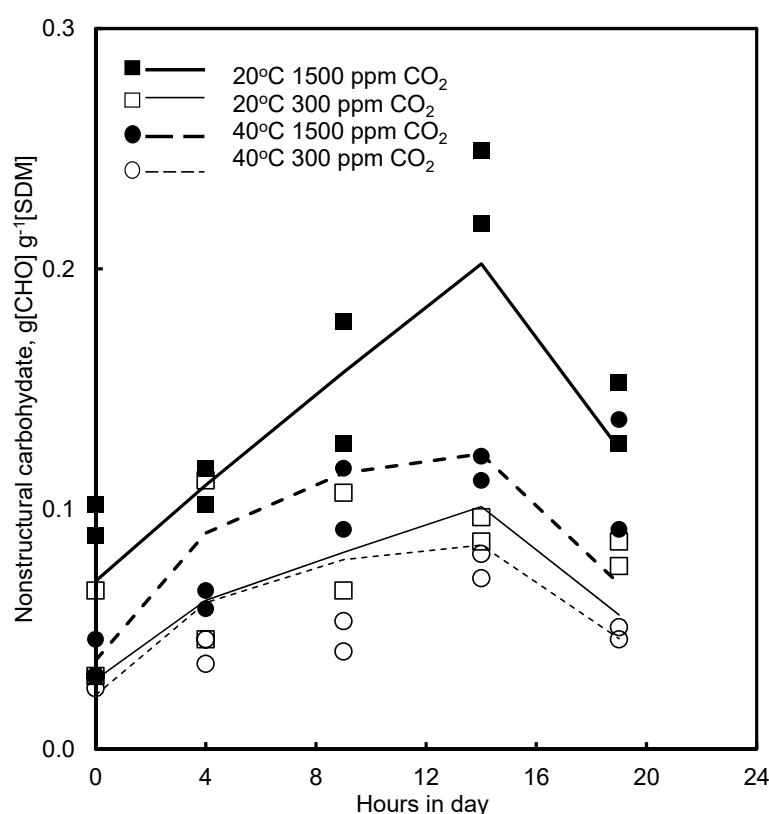183   actual values was R^2=0.78 to predict NSC and R^2=0.84 to predict RGR. The steady-state

184

185

186   Figure 7. Diurnal variation in NSC observed for melon grown at 20 and 40℃ day

187   temperatures, and at 300 and 1500 μmol[CO_2] mol^{-1} [18]. Symbols are observations from two

188   harvests, at 11 and 22 days of treatment pooled together. Lines are predictions from the
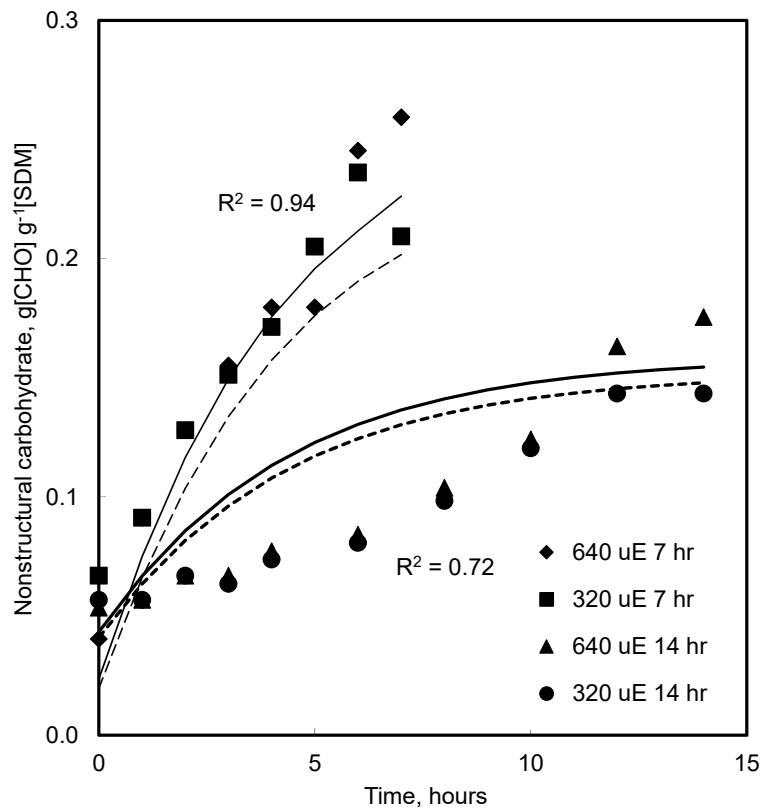
189   dynamic model.

190

191   Figure 8. Non-structural carbohydrate content of 'Amsoy' soybean grown under 7- or 14- h

192   day lengths and 320 or 640 μmol[PAR] m^{-2} s^{-1} [27]. Symbols are data and lines are

193   predictions of the dynamic model.

194

195   model could only predict NSC if the reserve carbohydrate had a term for CO_2 concentration,

196   with minimum values of NSC higher at 1500 than 300 umol[CO_2] mol^{-1}, at both 20 and 40°C

197   day temperatures.

198   The effect of day length and irradiance on NSC and RGR was predicted for soybean

199   (*Glycine max*) grown under 7- or 14- h day lengths and 320 or 640 μmol[PAR] m^{-2} s^{-1} [27].

200   The maximum rate of photosynthesis per unit leaf area of soybean occurred under 7-h

201   photoperiod, but the maximum rate per gram SDM occurred under the 14-h photoperiod [27].

202   Photosynthesis on a per leaf area basis was higher under high light. To account for this in the

203   dynamic model, a higher leaf area ratio was used for plants growing under 7-h than 14-h day

204   length. Values of λ were 32 and 38 m^2 kg^{-1}[SDM] under 7 h photoperiod, and 19 and 24 m^2

205   kg^{-1}[SDM] under 14-h photoperiod, for 640 and 320 μmol[PAR] m^{-2} s^{-1}, respectively. The

206   optimum temperature for photosynthesis was τ = 27°C, as for melon. Under a 7-h

207   photoperiod, the NSC values predicted by the dynamic model were similar to those observed

208   (Fig. 8). Under a 14-h photoperiod, the values of NSC predicted were more than observed,

209   except at dawn and dusk. Due to changes in λ, the observed and predicted NSC were similar

210   at 320 and 640 μmol[PAR] m^{-2} s^{-1} under the two day lengths. The correlation between

211   predicted and actual NSC values were R^2=0.94 and R^2=0.72, under 7- and 14-h photoperiods,

212   respectively. The lower NSC seen within the 14-h photoperiod may be a by-product of the

213   experimental methods. The model predicted growth rates of 0.31 vs 0.26 g g^{-1} d^{-1}, compared

214   to actual net assimilation rates of 0.28 vs 0.19 g g^{-1} d^{-1}, under 14- compared to 7-h

215   photoperiods at 640 μmol m^{-2} s^{-1}[PAR] [27]. There was little difference due to light intensity.

216

217   **5. DISCUSSION**

218   **Temperature effects on respiration**

219   Some features of fitting the model to results for prolonged respiration of tomato in

220   darkness agreed with the reported data and with standard intuition, but some did not. Dark

221   respiration in tomato, and bean under both high- and low-light pre-treatment, were well fit

222   with an exponential temperature dependence (Figs. 2 and 3). The plateau in respiration under

223   high NSC and cool temperature was as expected from Eqn. [13]. The initial substrate in bean

224   was set to 0.35 and 0.08 g[CHO] g^{-1}[SDM], for high- and low-light pre-treatment,

225   respectively. The initial value for high light was slightly greater than that published [14]. The

226   value for low light ensured that respiration had no plateau (Fig. 3 lower two curves). Breeze

227   and Elston [11] gave no procedure for measuring TNC, so the values may have changed from

228   one experiment to the next. The values of α_D were the same for tomato and bean.

229   The temperature dependence of growth respiration, ζ, was greater than that of

230   maintenance, **θ,** for tomato, and the same values was used for all other species (Table 1). The

231   values were equivalent to $\mathbf{Q_{10}}$ = 3 for growth and $\mathbf{Q_{10}}$ = 2 for maintenance. Thus, growth

232   enhanced by high light at higher temperatures. At sufficiently high temperature, growth was

233   inhibited by photosynthesis and the lack of NSC. Although some scientists think there is a

234   temporal effect of temperature on maintenance respiration, I found a $\mathbf{Q_{10}}$ = 2 for maintenance

235   of tomato over the range of 10 to 36°C. It is not clear if the temperature dependence of

236   growth respiration continues to increase above the point where NSC limits growth.

237   **Dependence of photosynthesis**

238   About one half of the dynamic model pertains to photosynthesis, the function that

239   supplies NSC for growth. I used non-interacting single-argument functions for light,

240   temperature and CO$_2$ concentration in Eqn. (3), all of them non-linear. More complex forms,

241   based on biochemistry of photosynthesis contain interactions between the effects of the

242   environmental factors [8]. Compared to the more complicated function, the form I used gave

243 a sum of squares from regression for tomato of $R^2 = 0.94$, compared to $R^2 = 0.97$ with the

244 Farquhar model. I decided to use the simpler model when predicting photosynthesis for other

245 species.

246   In the steady-state model, photosynthesis inhibition was determined by the minimum

247 daily NSC. In the dynamic model, photosynthesis inhibition was affected hour by hour, as

248 NSC varied over the day. This had a negative effect on photosynthesis and growth,

249 particularly for young tomato seedlings of [30]. A large fraction of photosynthesis must be

250 inhibited to predict NSC accurately under demand-limited conditions. Relatively little

251 inhibition of photosynthesis is required to predict growth under supply-limited conditions.

252 This combination could be achieved only by relating inhibition to the minimum NSC content

253 over the diurnal cycle, rather than using NSC hour by hour during the day. This agrees with

254 the data of Krapp and Stitt [26] on the increase of starch and photosynthetic inhibition in

255 spinach leaf discs.

256 **Values for n_0**

257   The parameter related to maximum growth, n_0, varied among the two studies of tomato.

258 The value used to fit the data of Gary et al. [14] was smaller than that used to fit the data for

259 tomato seedlings [30], which were in an earlier stage of growth. Acock et al. [18] found a

260 slower RGR but higher NSC for melon plants that were 10 days older, when grown under the

261 same conditions. This was predicted with a lower value for n_0 for older plants. Other

262 observations in lettuce [32, 33] noted that older and larger plants had slower growth but

263 higher NSC than younger and smaller plants. These observations are not reconciled with the

264 dynamic model, which would predict a lower NSC related to self-shading and reduced light

265 intensity per unit leaf area in larger plants. These observations may show that a smaller

266 fraction of total biomass is growing in larger compared to smaller plants.

267   Another explanation concerns the whole-plant nature of the dynamic model. NSC is

268 found in all plant organs, but in some organs such as stems and tubers, the NSC appears to be

269 in relatively long-term storage, and not immediately used for metabolism. The NSC in leaves

270 is usually turned over with a half-life of a few hours, due to metabolism and translocation to

271 other parts of the plant. (I thank Stephane Adamowicz for this insight.) Young seedlings have

272 a large fraction of biomass in leaves compared to older plants. Thus, a larger fraction of NSC

273 may be metabolically active in young, compared to older, plants. A consequence of this

274 argument is that n_0 should be scaled inversely with plant size to emulate the changing relation

275 between NSC and growth rate. This change in n_0 would correspond to the proportion of

276 actively growing tissue as a fraction of total biomass.

Starch and starch-less plants

Starch increases in leaves in the day and decreases in the night in a roughly linear fashion [19]. The dynamic model predicted a nonlinear response, with faster use of NSC at dusk and slower use at dawn (Eqn. 13). Growth rates may be responding to soluble sugars rather than NSC. The relationship between NSC and growth in the day, $\boldsymbol{\alpha_L}$, was much higher for the starch-less Arabidopsis, **pgm,** than the starch synthesizing, **COL0** [31]. There may be two state storage variables; starch and sugar. The dynamic model using NSC worked well for whole plants, because the NSC in parts other than leaves took a while to equilibrate between sugar and starch, and thus affect respiration and growth in all parts.

CO$_2$ and growth

Carbon dioxide enrichment increased growth of melon but had less effect on NSC. The highest NSC was at 20°C and 1500 µmol mol^{-1} CO$_2$ (Fig 7), while the fastest growth was at 40°C and 1500 µmol[CO$_2$] mol^{-1} [18]. Plants under 300 µmol[CO$_2$] mol^{-1} did not have enough NSC for rapid growth at either 20 or 40°C. Inhibition of photosynthesis is often seen in plants under CO$_2$ enrichment, especially when CO$_2$ increases NSC. The high value of NSC under 1500 µmol[CO$_2$] mol^{-1} resulted in an predicted inhibition of photosynthesis of $\boldsymbol{\beta}$=0.108 and $\boldsymbol{\beta}$=0.044 g[CHO] g^{-1}[SDM] h^{-1}, at 20°C compared to 40°C, respectively. The values under 300 µmol[CO$_2$] mol^{-1} did not differ as much, $\boldsymbol{\beta}$=0.038 and $\boldsymbol{\beta}$=0.024 g[CHO] g^{-1}[SDM] h^{-1}, at 20 and 40°C. Thus, the dynamic model predicted greater inhibition of photosynthesis under high compared to low CO$_2$. One value of the dynamic model was that it predicted an inhibition of photosynthesis due to CO$_2$ enrichment.

NSC and growth

The dynamic model retained some NSC at the end of the dark period. This 'reserve carbohydrate' was not specified independently of supply and demand, as in the steady-state model [9], where the reserve carbohydrate was immune to metabolism, and appeared to be related to light intensity or photosynthesis. The dynamic model predicted differences in NSC at dawn, primarily due to differences in light intensity that existed at dusk. The NSC was metabolized at a faster rate in the dark for plants with more NSC at dusk, but it never became equal to that in plants with less NSC. Thus Eqn. [16], that limited growth through the dark period, also conserved NSC, even under conditions when the temperature dependence of growth by itself, ($\mathbf{n}\{T\}-\mathbf{m}\{T\}$), predicted all carbohydrate would be consumed.

Some predictions of NSC from the dynamic model were greater than those observed for Arabidopsis plants under a long photoperiod (Table 3 and Fig. 5) [31] and for soybean under

310 two day lengths (Fig. 8) [27]. However, the dynamic model predicted the correct NSC at the

311 end of the day. I do not know if the errors within the daily cycle were due to the data or due

312 to the model. In any case at any point in the diurnal cycle, NSC in short photoperiod plants

313 should be less than in long photoperiod plants, as long as sugar metabolism is not inhibited

314 early in the day.

315

316 **6. SUMMARY**

317 A dynamic model of carbohydrate metabolism and growth was tested under various

318 conditions. The dynamic model predicted respiration for plants in extended darkness [11, 14].

319 The dynamic model also predicted a better NSC of tomato under two light levels and various

320 temperatures from 9 to 36°C [30], compared to a steady-state model [9]. Parameters of the

321 dynamic model used to fit tomato also fit data on NSC in starch-synthesizing and starch-less

322 arabidopsis [31], using NSC as a replacement for sugar or starch. The predictions of the

323 model also fit the CO_2 and temperature response of melon [18], and day length response of

324 soybean [27]. The model was based on data for seedling plants, in which leaf area ratio was

325 specified per unit structural dry matter. Some other parameters would be more important for

326 studies of larger plants, such as the effect of leaf area index on photosynthesis [2, 3], and the

327 proportion of the plant that is growing.

328

329 **7. ACKNOLEDGEMENTS**

330 I thank Ido Seginer for his contributions to this manuscript describing a dynamic

331 carbohydrate supply and demand model of vegetative growth.

332

333 **8. EXPERIMENTAL METHODS**

334 **Respiration in Prolonged Darkness**

335 Two studies followed respiration in prolonged darkness, to understand NSC use without

336 photosynthesis. Ten-week old tomato plants (*Solanum lycopersicon*) were grown under either

337 high or low light conditions, 1000 or 200 μmol[PAR] m^{-2} s^{-1} , before being put in prolonged

338 darkness [14]. At the beginning of darkness, the values of NSC were 0.236 and 0.120

339 g[CHO] g^{-1}[SDM], under high light and low light, respectively. Another set of values comes

340 from work of Breeze and Elston [11] on bean (*Vicia faba)*. Dark respiration was followed for

341 14-h in plants that were first adapted to high or low light at 20°C. These pre-treatments were

342 200 or 35 W[PAR] m^{-2} for 18-h light, 6-dark, 18-h light applied to 4 to 7 week old plants.

343 The mean NSC after pre-treatment was reported as 0.31 and 0.24 g[CHO] g^{-1}[SDM] under

344 high and low light, respectively.

Effect of temperature and light

346   Gent [30] examined the response of tomato seedlings 'Sonato' to a wide range of

347 temperatures under controlled environment conditions with a 12-h photoperiod. Light and

348 temperature were controlled, and CO_2 concentration was 400-450 μmol[CO_2] mol^{-1}. There

349 were 8 experimental cycles, each at a different temperature, ranging from 9 to 36°C. Day and

350 night temperatures were the same. Within each experiment there were two light intensities,

351 averaging 110 and 370 μmol[PAR] m^{-2} s^{-1}. The environment was imposed 5 to 18 days after

352 germination, first harvest was 2 to 5 days later, and final harvests were at dusk and dawn, 3 to

353 11 days following the first harvest. Total dry mass was determined for all harvests, and leaf

354 area in the final harvest only. The relative growth rate was determined from initial and final

355 harvests. The NSC, equal to starch plus soluble carbohydrate per g[TDM], was determined at

356 dusk and dawn on the final day of the experiment. Observed values were recalculated from

357 Figures 1 and 4 of Gent [30].

Starch and Starchless mutants of Arabidopsis

359   Data from Gibon et al. [31] were used to find NSC for various times within a 24 h cycle

360 for *Arabidopsis thaliana* plants with and without starch synthesis. They compared NSC in a

361 wild ecotype, **COL0,** and **pgm,** a line without starch synthesis. The plants were grown in soil

362 as in Thimm et al. [34], under various photoperiods of 140 μmol[PAR] m^{-2} s^{-1} within a 24 h

363 diurnal cycle. I assumed the temperature was 25°C and CO_2 was 380 μmol[CO_2] mol^{-1}.

364 Vegetative plants were harvested and transferred to liquid nitrogen for analyses. Observed

365 values came from Figures 4, 5, and 6 of Gibon et al. [31].

Effect of CO_2 and Photoperiod

367   A dataset for melon (*Cucumis melo*) 'Haogen' [18] was used to compare the effects of

368 temperature and CO_2 concentration on growth. Before treatment, the conditions were 208

369 μmol[PAR] m^{-2} s^{-1} under a 14-h photoperiod, 30°C temperature and ambient CO_2.

370 Experimental treatments were applied at 25- or 35-d after sowing. Light and photoperiod

371 were as during the pre-treatment period. Day-time temperatures were 20 or 40°C, with a

372 common night-time temperature of 20°C. Plants were grown under either 300 or 1500

373 μmol[CO_2] mol^{-1} in each temperature regime. Biomass, leaf area, and NSC concentrations

374 were determined in plants harvested 11 d after start of the treatments. Relative growth rates

375 used here are for the younger plants. Specific leaf area was calculated from analysis of

376 temperature and CO_2 concentration effects, and converted to structural leaf area ratio using a

377 constant proportion of 0.6. Observed values were obtained from Figure 2 of Acock et al. [18].

378   Data of Chatterton and Silvius [27] were used to determine the effect of day length and

379   irradiance on soybean (*Glycine max*) 'Amsoy'. Young plants were placed in 1.5 L pots filled

380   with vermiculite and grown at an air temperature of 27ºC under irradiance of 320 or 640

381   μmol[PAR] m^{-2} s^{-1}. The two photoperiods were 7- and 14-h within a 24-h day length. The

382   CO_2 concentration was assumed to be 330 μmol[CO_2] mol^{-1} . Rates of photosynthesis and

383   determination of NSC were from Table 1 and Figure 4 of Chatterton and Silvius [27]. Dry

384   matter was converted to SDM by subtracting NSC per unit DM, and NSC was recalculated

385   from SDM.

386   The conditions used to simulate all these data are shown in Table 2.

387

388   APPENDIX A

389   Curly brackets, {}, are used exclusively for arguments of functions

390   ***Abbreviations***

391   **C**   NSC content   g[CHO] m^{-2}[ground], g[CHO] g^{-1}[SDM]

392   **c**   Rate of change of **C**   g[CHO] m^{-2}[ground] h^{-1}, g[CHO] g-1[SDM] h^{-1}

393   **C$_a$**   Carbon dioxide concentration   μmol[CO$_2$] mol^{-1}[air]

394   **C$_d$**   Minimum NSC content   g[CHO] g^{-1}[SDM]

395   *f*   Response of photosynthesis to light   −

396   **g**   Growth respiration rate   g[CHO] m^{-2}[ground] h^{-1}, g[CHO] g^{-1}[SDM] h^{-1}

397   *h*   Response of photosynthesis to temperature   −

398   **i**   Photosynthesis inhibition rate   g[CHO] m^{-2}[ground] h^{-1}, g[CHO] g^{-1}[SDM] h^{-1}

399   *k*   Response of photosynthesis to carbon dioxide concentration   −

400   *L*   Light flux   μmol[PAR] m^{-2}[leaf] s^{-1}

401   **m**   Maintenance respiration rate   g[CHO] m^{-2}[ground] h^{-1}, g[CHO] g^{-1}[SDM] h^{-1}

402   **m$_0$**   Maintenance respiration at 0 ºC g[CHO] m^{-2}[ground] h^{-1}, g[CHO] g^{-1}[SDM] h^{-1}

403   **n**   Maximum rate of metabolism   g[CHO] m^{-2}[ground] h^{-1}, g[CHO] g^{-1}[SDM] h^{-1}

404   **n$_0$**   Rate of metabolism at 0 ºC   g[CHO] m^{-2}[ground] h^{-1}, g[CHO] g^{-1}[SDM] h^{-1}

405   *P$_{max}$*   Maximum rate of photosynthesis   g[CHO] m^{-2}[leaf] h^{-1}

406   *p*   Specific photosynthesis rate   g[CHO] m^{-2}[leaf] h^{-1}

407   **p**   Potential gross photosynthesis rate g[CHO] m^{-2}[ground] h^{-1}, g[CHO] g^{-1}[SDM]

408   h^{-1}

409   *Q$_{10}$*   Temperature quotient: ratio of reaction rates at 10K difference   −

410   **S**   Structural dry matter content   g[SDM] m^{-2}[ground]

411   **s**   Structural growth rate   g[SDM] m^{-2}[ground] h^{-1}, g[SDM] h^{-1}

412   *T*   Temperature   K

413   *t*   Time   h

414   **α$_D$**   Response of growth to NSC in the dark   h^{-1}

415   **α$_L$**   Response of growth to NSC in the light   h^{-1}

416   ***β***   Factor relating photosynthesis inhibition to NSC   g[SDM] g^{-1}[CHO]

417   *γ*   Light intensity at half maximum photosynthesis   μmol[PAR] m^{-2}[leaf] s^{-1}

418   ***δ***   CO$_2$ concentration at half maximum photosynthesis   μmol[CO$_2$] mol^{-1}[air]

419   **ε**   Growth conversion efficiency   −

420	ζ	Exponential temperature coefficient for maximum metabolism	K^{-1}
421	κ	Sensitivity of photosynthesis to temperature	K^{-2}
422	τ	Threshold temperature for photosynthesis	K
423	Λ	Total leaf area index	m^2[leaf] m^{-2}[ground]
424	λ	Ratio of leaf area to structural dry matter	m^2[leaf] kg^{-1}[SDM]
425	θ	Exponential temperature coefficient for maintenance respiration	K^{-1}
426			

427   Table 2. Environmental conditions used to simulate growth and non-structural carbohydrate in various crops.

			[30]	[31]	[18]	[27]
	Units	Symbol	Tomato	Arabidopsis	Melon	Soybean
Light	$\mu mol[PAR]$	L	87 – 134	140	208	320
	$m^{-2}\,s^{-1}$		325 - 409			640
Temperature	ºC	T	9 - 36	25	20, 40	27
Carbon dioxide	$\mu mol[CO_2]$	C_a	450	380	300	330
concentration	mol^{-1}				1500	
Day length	h		12	6 - 20	14	7, 14
Leaf area ratio	$m^2\,kg^{-1}$	λ	32.3 to 47.9	18.5	21, 30	18, 20
	[SDM]		25.5 to 38.5		19, 27	36, 40

428

REFERENCES

1. Alagarswamy, G, Boote K.J., Allen L.H., Jones J.W. (2006) Evaluating the CROPGRO-Soybean model ability to simulate photosynthesis response to carbon dioxide levels. Agronomy J. 98, 34-42.

2. Kim, S-H., Y. Yang, D.L. Timlin, D.H. Fleischer. A. Dathe, R.R. Reddy, and K. Staver. 2012. Modeling temperature responses and biomass in Maize with MAIZSIM. Agronomy J. 104:523-1537.

3. Timlin, D., S.M. Lutfor Rahman, J. Baker, V.R. Reddy, D. Fleisher, and B. Quebedeaux. 2006. Whole plant photosynthesis, development, and carbon partitioning in potato as a function of temperature. Agronomy J. 98:1195-1203.

4. Verdoodt, A., E. Van Ranst, and L. Ye. 2004. Daily simulation of potential dry matter production of annual field crops in tropical environments. Agronomy J. 96:1739-1753.

5. Scaife, M.A. 1973. The early relative growth rates of six lettuce cultivars as affected by temperature. Annals Applied Biology 74:119-128.

6. Kemp, D.R., and W.M. Blacklow. 1980. Diurnal extension rates of wheat leaves in relation to temperatures and carbohydrate concentrations of the extension zone. J Experimental Botany 31:821-828.

7. Yamori, W., K. Noguchi, K. Hikosaka, and I. Terashima. 2010. Phenotypic plasticity in photosynthetic temperature acclimation among crop species with different cold tolerances. Plant Physiology 152:388-399.

8. Farquhar, G.D., S. von Caemmerer, and J.A. Berry. 1980. A biochemical model of photosynthetic CO_2 assimilation in leaves of C_3 species. Planta 149:78-90.

9. Gent, M.P.N., and I. Seginer. 2012. A carbohydrate supply and demand model of vegetative growth: Response to temperature and light. Plant, Cell, and Environment 35, 1274-1286

10. Seginer, I., and M.P.N. Gent. 2014. Short and long term vegetative growth response to temperature, interpreted by the dynamics of a carbohydrate storage. Scientia Hort 171:14-26.

458   11. Breeze, V., and J. Elston. 1978. Some effects of temperature and substrate content

459   upon respiration and the carbon balance of field beans (*Vicia faba* L.). Annals of

460   Botany 42:863-876.

461   12. Baysdorfer, C., R.D. Warmbrodt, and W.J. VanDerWoude. 1988. Mechanisms of

462   starvation tolerance in pearl millet. Plant Physiology 88:1381-1385

463   13. Brouquisse, R., J.P. Gaudillère, and P. Raymond. 1998. Induction of a carbon-

464   starvation-related proteolysis in whole maize plants submitted to light/dark cycles

465   and to extended darkness. Plant Physiology 117:1281–1291.

466   14. Gary, C., P. Baldet, N. Bertin, C. Devaux, and M. Tchamitchian. 2003. Time-course

467   of tomato whole-plant respiration and fruit and stem growth during prolonged

468   darkness in relation to carbohydrate reserves. Annals of Botany 91:1-10.

469   15. Devaux, C., P. Baldet, J. Joubes, M. Dieuaide-Noubhani, D. Just, C. Chevalier, and

470   P. Raymond. 2003. Physiological, biochemical and molecular analysis of sugar-

471   starvation responses in tomato roots. J. Experimental Botany 54:1143–1151

472   16. Moser, L.E., J.J Volenec, and C.J. Nelson. 1982. Respiration, carbohydrate content,

473   and leaf growth of tall fescue. Crop Science 22:781-786.

474   17. Hendershot, K.L., and J.J. Volenec. 1989. Shoot growth, dark respiration, and

475   nonstructural carbohydrates of contrasting alfalfa genotypes. Crop Science 29:1271-

476   1275.

477   18. Acock, B., M.C. Acock, and D. Pasternak. 1990. Interactions of CO2 enrichment

478   and temperature on carbohydrate production and accumulation in muskmelon

479   leaves. J. Amer. Soc. Hort. Sci. 115:525-529.

480   19. Fondy, B.R., D.R. Geiger, and J.C. Servaites. 1989. Photosynthesis, carbohydrate

481   metabolism, and export in *Beta vulgaris* L. and *Phaseolus vulgaris* L. during square

482   and sinusoidal light regimes. Plant Physiology 89:396-402

483   20. Krapp, A., and M. Stitt. 1995. An evaluation of direct and indirect mechanisms for

484   the "sink-regulation" of photosynthesis in spinach: Changes in gas exchange,

485   carbohydrates, metabolites, enzyme activities and steady-state transcript levels after

486   cold-girdling source leaves. Planta 195:313-323.

487   21. Ayari, O., M. Dorais, and A..Gosselin. 2000. Daily variations in photosynthetic

488   efficiency of greenhouse tomato plants during winter and spring. J. Amer. Soc.

489   Hort. Sci. 125:235-241.

490   22. Geiger, D.R., and J.C. Servaites. 1994. Diurnal regulation of photosynthetic carbon

491   metabolism in C_3 plants. Annual Reviews of Plant Biology 45:235–256.

492   23. Geiger, D.R., J.C. Servaites, and M.A. Fuchs. 2000. Role of starch in carbon

493   translocation and partitioning at the plant level. Australian Journal of Plant

494   Physiology 27:571–582.

495   24. Gerhardt, R., M. Stitt, H.W. Heldt. 1987. Subcellular metabolite levels in spinach

496   leaves: Regulation of sucrose synthesis during diurnal alterations in photosynthetic

497   partitioning. Plant Physiol 83:399-407

498   25. Matt, P., U. Schurr, A. Krapp, and M. Stitt. 1998. Growth of tobacco in short day

499   conditions leads to high starch, low sugars, altered diurnal changes of the Nia

500   transcript and low nitrate reductase activity, and an inhibition of amino acid

501   synthesis. Planta 207:27–41.

502   26. Zeeman, S.C., F. Northrop, A.M. Smith, and T. ap Rees. 1998. A starch-

503   accumulating mutant of *Arabidopsis thaliana* deficient in a chloroplastic starch-

504   hydrolysing enzyme. Plant Journal 153:57–365.

505   27. Chatterton, N.J., and J.E . Silvius. 1981. Photosynthate partitioning into starch in

506   soybean leaves: irradiance level and daily photosynthetic period duration effects.

507   Plant Physiology 67:257–260.

508   28. Caspar, T., S.C Huber, and   C.R . Somerville. 1985. Alterations in growth,

509   photosynthesis and respiration in a starch deficient mutant of *Arabidopsis thaliana*

510   (L.) Heynh deficient in chloroplast phosphoglucomutase. Plant Physiology 79:11–

511   17.

512   29. Lin, T.P., T. Caspar, C.R. Somerville, and J. Preiss. 1988. A starch deficient mutant

513   of Arabidopsis thaliana with low ADP glucose pyrophosphorylase activity lacks one

514   of the 2 subunits of the enzyme. Plant Physiology 88:1175–1181.

515   30. Gent, M.P.N. 1986. Carbohydrate level and growth of tomato plants. II. The effect

516   of irradiance and temperature. Plant Physiology 81:1075-1079.

517   31. Gibon, Y., O.E.Blasing, N. Palacios-Rios, D. Pankovic, J.H.M.Hendriks, H. Fisahn,

518   M. Hohne,   M. Genther, and M. Stitt. 2004. Adjustment of diurnal starch turnover

519   to short days: depletion of sugar during the night leads to a temporary inhibition of

520   carbohydrate utilization, accumulation of sugars and post-translational activation of

521   ADP-glucose pyrophosphorylase in the following light period. Plant Journal 39:847-

522   862.

523   32. Gent, M.P.N. 2012. Composition of hydroponic lettuce: Effect of time of day, plant

524   size, and season. J. Science in Food and Agriculture 92:542-550.

525   33. Van Iersel, M W. 2003. Carbon use efficiency depends on growth respiration,

526   maintenance respiration, and relative growth rate. A case study with lettuce. Plant,

527   Cell, and Environment 26:1441-1449

528   34. Thimm, O., O.E. Blaesing, Y. Gibon, A. Nagel, S. Meyer, P. Krueger, J. Selbig,

529   L.A. Mueller,   S.Y. Rhee, and M. Stitt. 2004. Mapman: a user-driven tool to

530   display genomics data sets onto diagrams of metabolic pathways and other

531   biological processes. Plant Journal. 37:914–939.

532   35. Penning de Vries, F.W.T, J.M. Witlage, D. Kremer. 1979. Rates of respiration and

533   structural growth in young wheat, ryegrass, and maize plants in relation to

534   temperature, water stress, and sugar concentration. Annals Botany 44:595-609.

535